Supporting Information

Trace Sn modified Zn catalysts for efficient CO_2 electroreduction to HCOOH

Rui Yang[a*], Hao Fu[a], Zimin Han[a], Guoqing Feng[a], Huaizhi Liu[a], Yangguang Hu[b*], Yiyin Huang[c*]

[a]School of Materials and Chemistry, Anhui Agricultural University, Biomass Molecular Engineering Center, Engineering Research Center for High-Performance Fiber Products for Automobile of Anhui Province, Hefei, 230036, P.R. China

[b]Hefei National Laboratory for Physical Sciences at the Microscale, iChEM, School of Chemistry and Materials Science, and National Synchrotron Radiation Laboratory, University of Science and Technology of China, Hefei, Anhui 230026, China.

[c]College of Physics and Energy, Fujian Normal University, Fujian Provincial Key Laboratory of Quantum Manipulation and New Energy Materials, Fuzhou, 350117, China

Corresponding author: ruiyang@ahau.edu.cn (R. Yang)

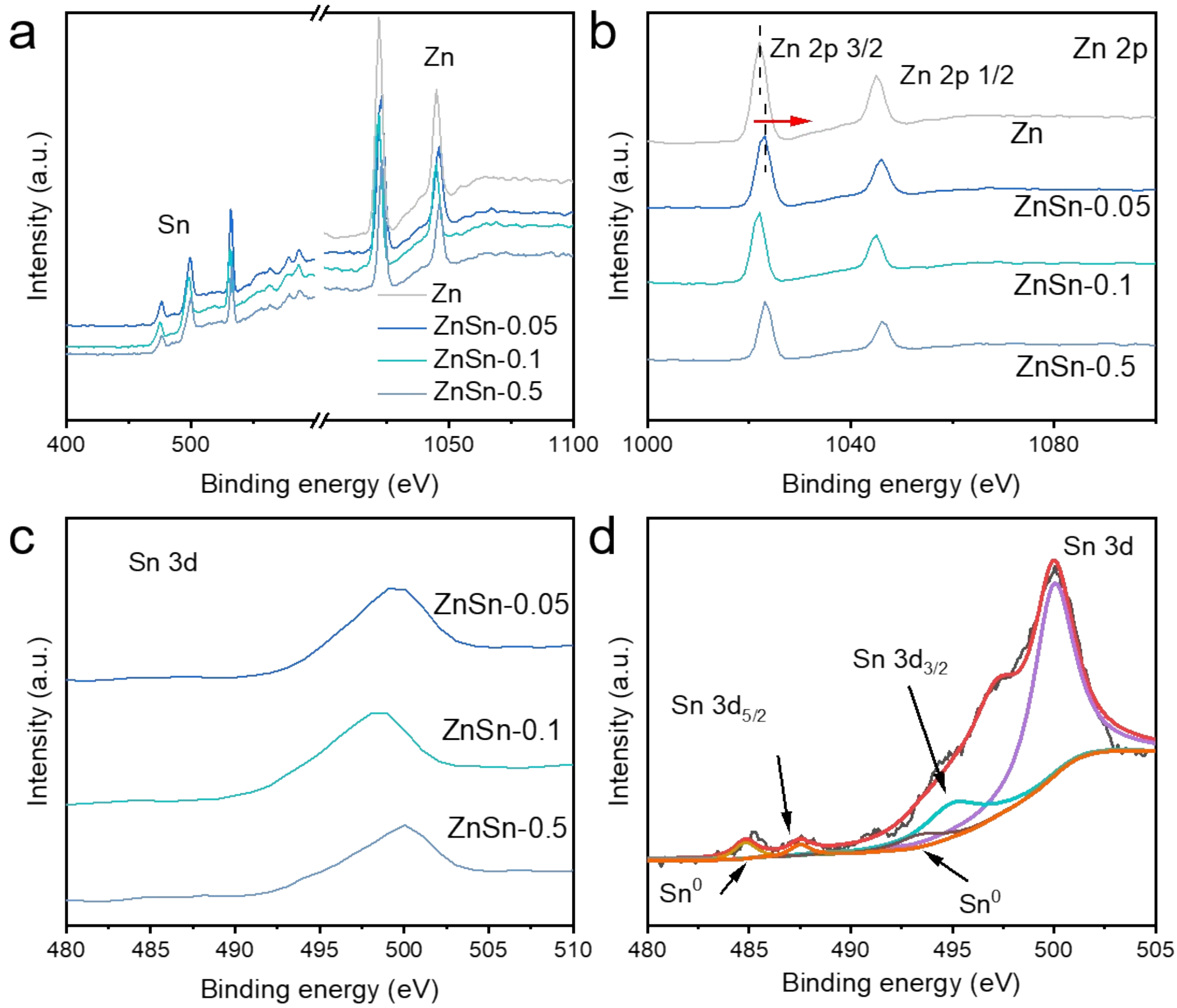

Figure S1. XPS for prepared materials and fine spectra of Zn and Sn.

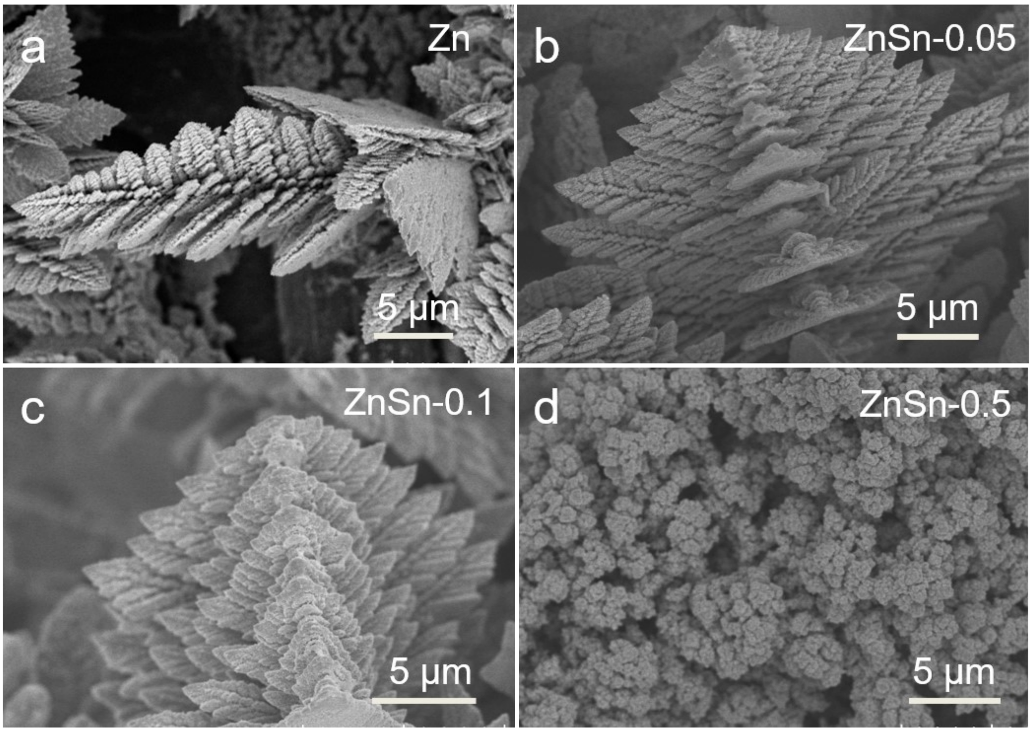

Figure S2. SEM images of Zn, ZnSn-0.05, ZnSn-0.1, and ZnSn-0.5.

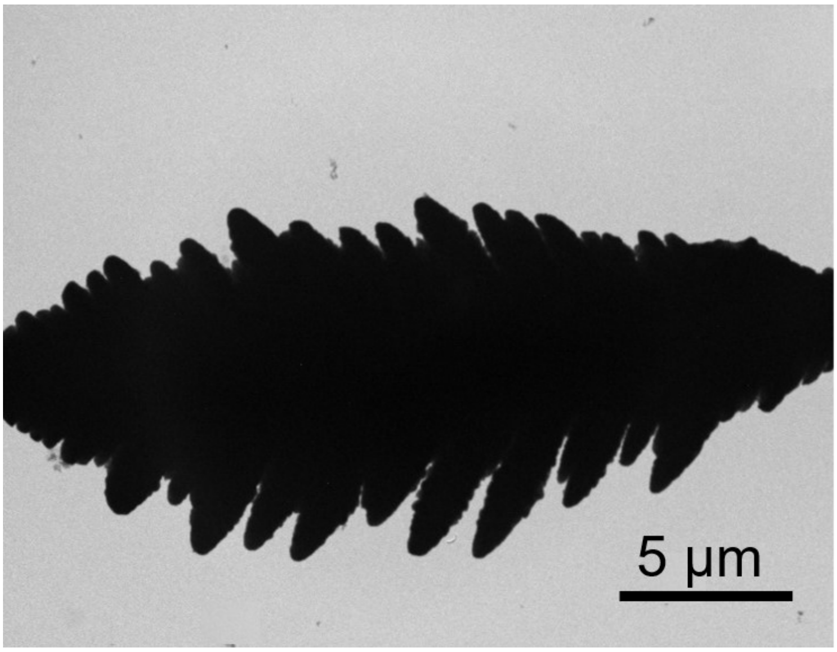

Figure S3. TEM image for ZnSn-0.05.

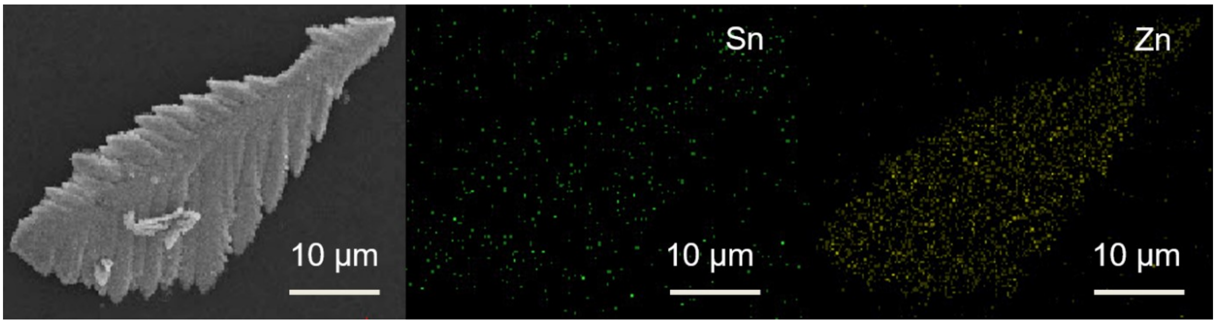

Figure S4. EDS for ZnSn-0.05 electrocatalyst.

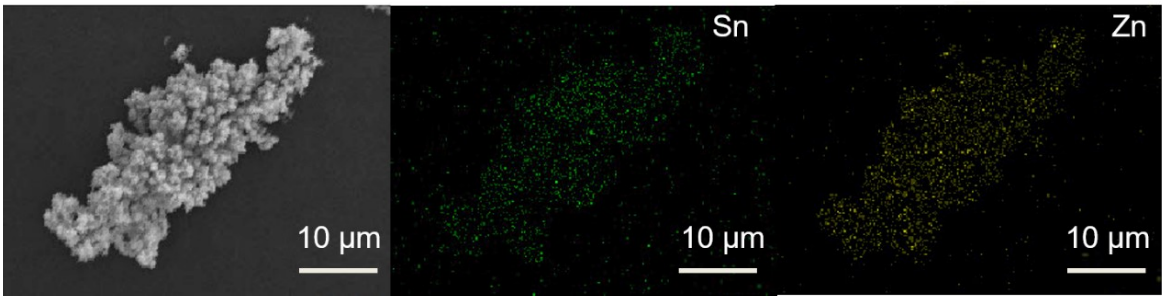

Figure S5. EDS for ZnSn-0.5 electrocatalyst.

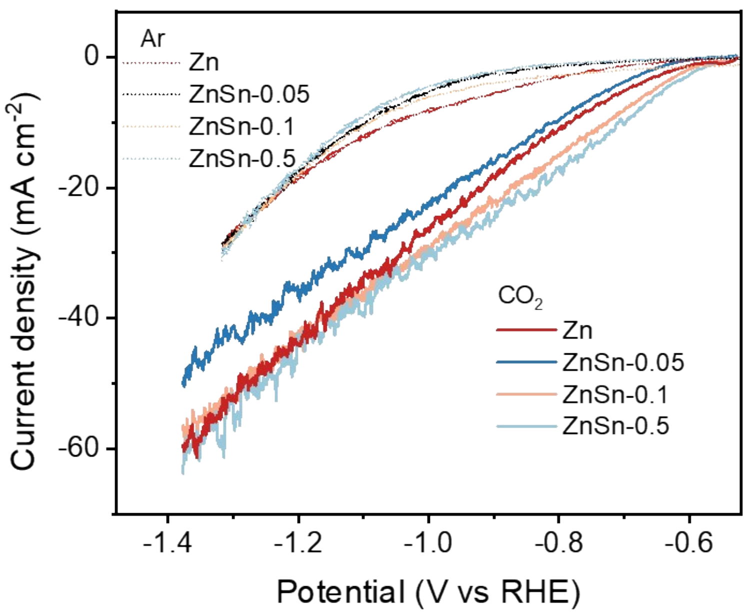

Figure S6. LSV curves of a series of Sn doped Zn materials saturated in CO_2 and Ar in 0.5 M $KHCO_3$ solution.

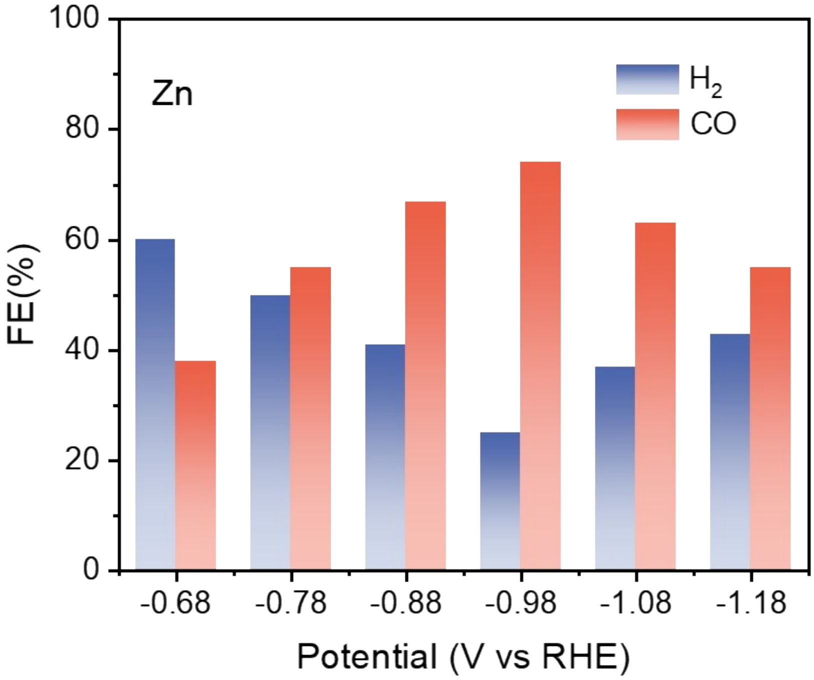

Figure S7. FE for Zn electrocatalyst toward CO_2RR.

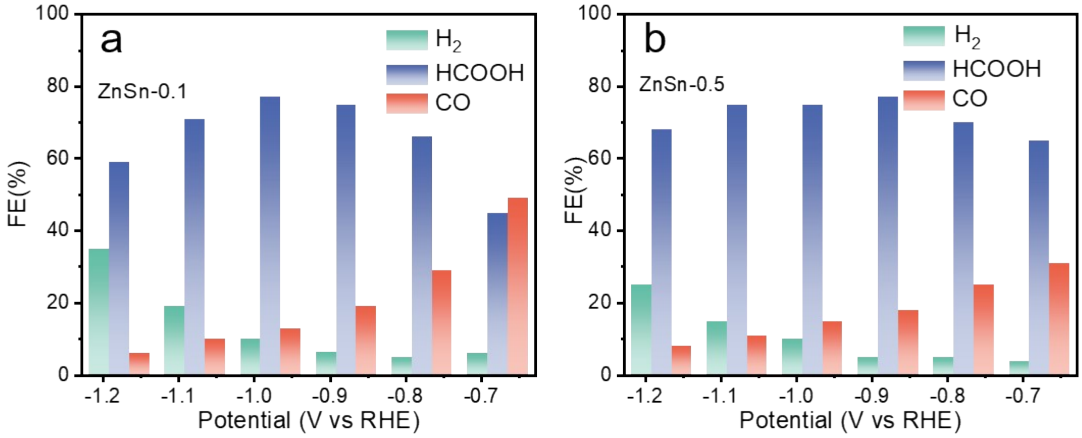

Figure S8. (a) FEs for ZnSn-0.1 and (b) ZnSn-0.5.

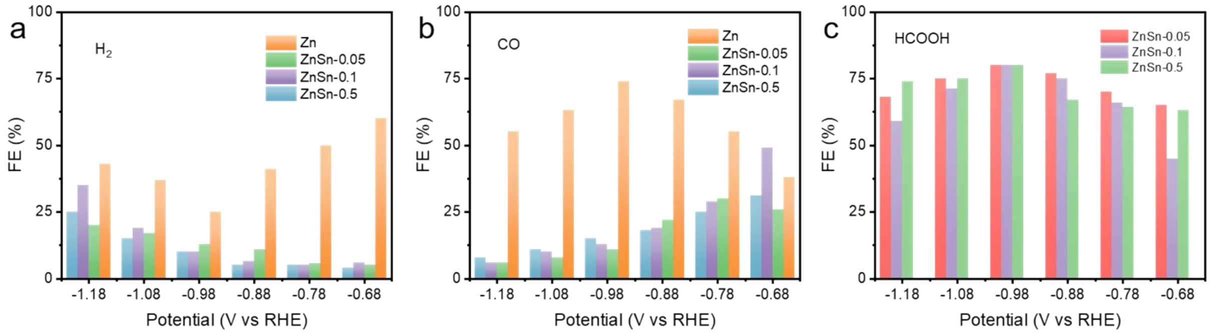

Figure S9. FEs for H_2, CO and HCOOH formation on prepared catalysts with different content of Sn.

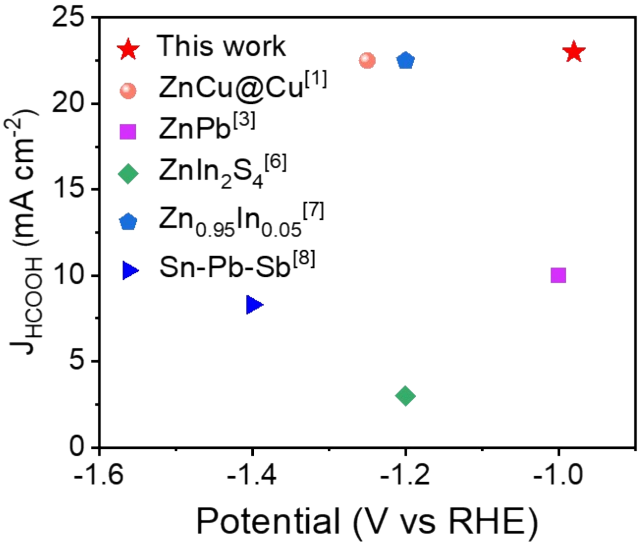

Figure S10. The comparison of corresponding HCOOH partial current density at maximum FE among various reported Zn-based electrocatalysts.

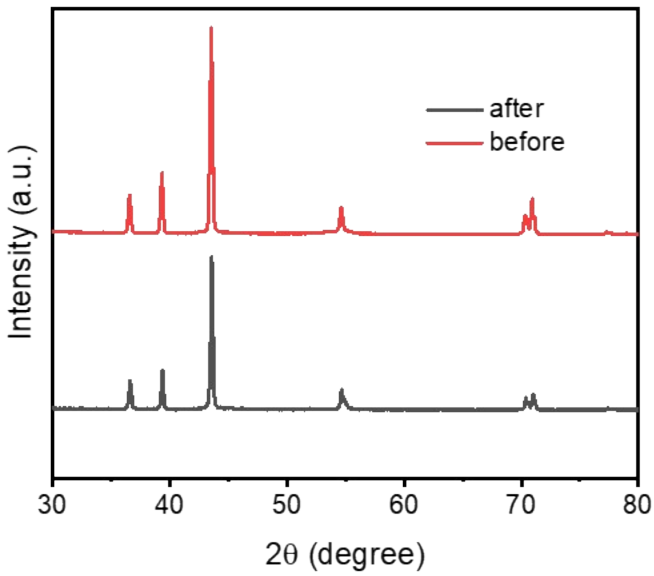

Figure S11. XRD pattern for ZnSn-0.05 before and after long-term electrolysis at at -0.88 V vs. RHE.

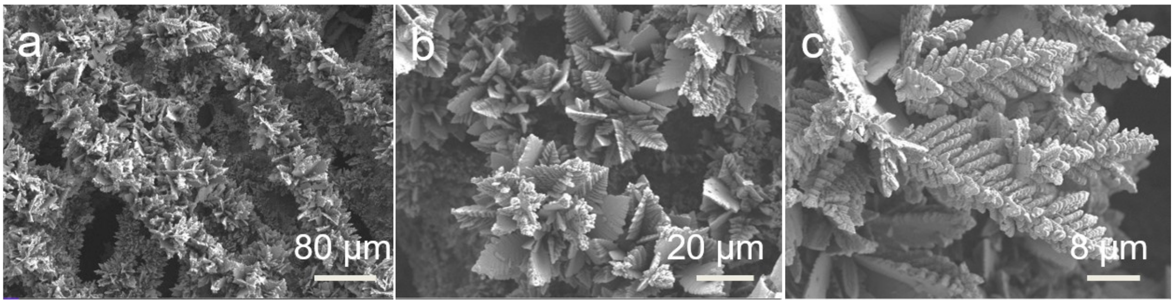

Figure S12. SEM image for ZnSn-0.05 after long-term electrolysis.

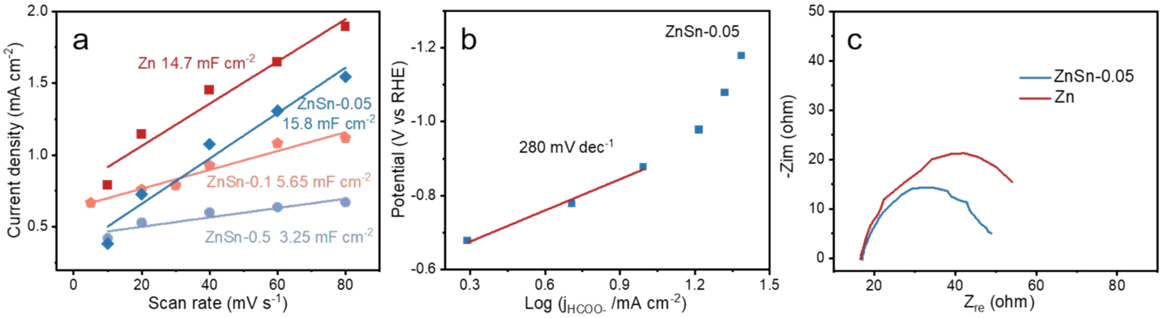

Figure S13. (a) Double-layer capacitance (Cdl) values for Zn, ZnSn-0.05, ZnSn-0.1, and ZnSn-0.5, (b) Tafel plot for producing $HCOO^-$, and (c) Nyquist plots for EIS analysis of ZnSn-0.05 and Zn.

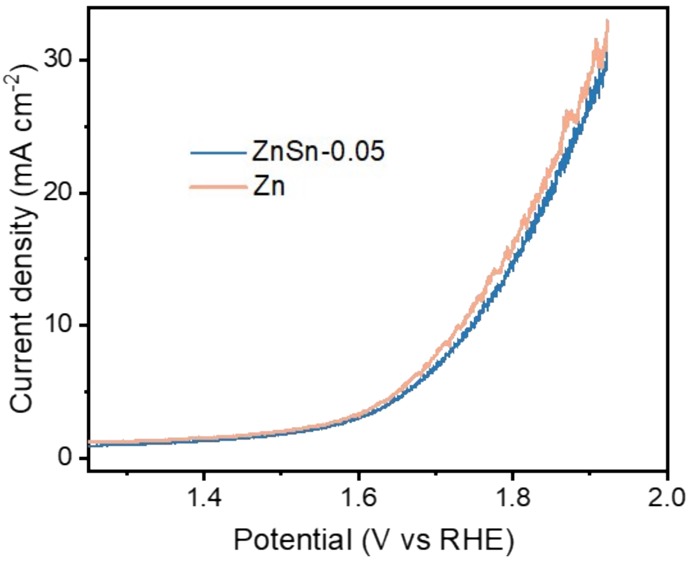

Figure S14. LSV curves for Zn and ZnSn-0.05 in 1 M KOH solution towards OER.

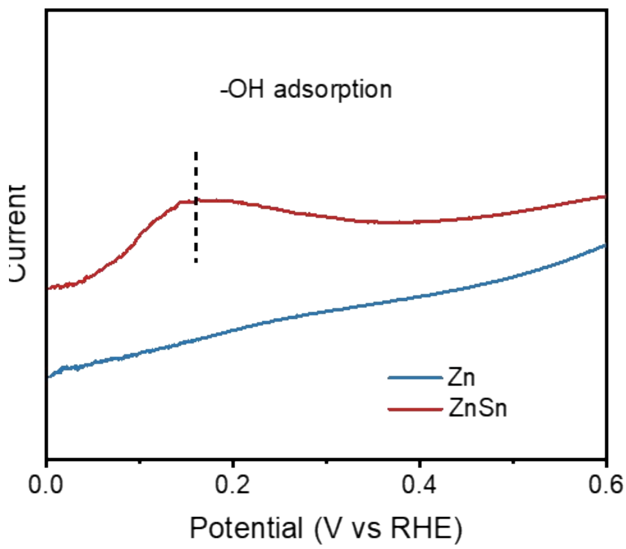

Figure S15. Single oxidative LSV scans in N_2-saturated 0.1 M NaOH solution of Zn and ZnSn.

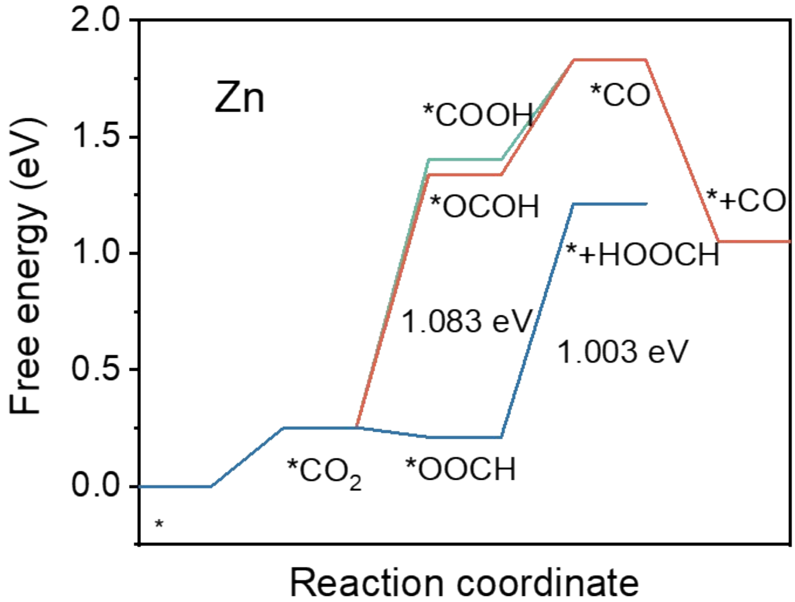

Figure S16. Free energy of CO_2RR into HCOOH/CO on Zn (002).

Table S1. Comparison of the activities Zn-based catalysts toward formate production

Catalysts	**Electrolyte**	**Potential (V vs RHE)**	**FE (%)**	**Stability (h)**	**Content of doping element (%)**	**Current density (mA cm^{-2})**	**Mass activity (mA mg_{doping}^{-1})**	**Mass FE (% mg_{doping}^{-1})**
ZnSn-0.05[this work]	0.5 M $KHCO_3$	-0.98	80	21	Sn-0.27	30	111.11	296.30
ZnCu@Cu[1]	0.5 M $KHCO_3$	-1.25	48.6	12	-	30	-	-
Zn_3Sn_2[2]	0.5 M $KHCO_3$	-1.1	96.7	12	Sn-39	30	0.76	2.47
ZnPb[3]	0.1M $KHCO_3$	-1.0	95	8	Pb-0.7	20	28.5	135.71
$ZnBi_3$[4]	0.1 M $KHCO_3$	-0.8	94	7	-	3.8	-	-
$Sn_{56.3}Pb_{43.7}$[5]	0.5 M $KHCO_3$	-1.4	80	none	-	56.25	-	-
$ZnIn_2S_4$[6]	0.1 M $KHCO_3$	-1.2	91	10	-	4.5	-	-
$Zn_{0.95}In_{0.05}$[7]	0.5 M $KHCO_3$	-1.2	95	1	In-8	22	2.75	11.875
Oxide-derived Sn-Pb-Sb[8]	0.1 M $KHCO_3$	-1.4	91	1.5	-	10	-	-
Sn-ZnO[9]	0.5 M $KHCO_3$	-1.2	80	11	Sn-1.02	60	58.8	78.43

Table S2. Carbon conversion efficiency (CCE) of prepared materials at -0.98 V vs RHE.

Sample	Zn	ZnSn-0.05	ZnSn-0.1	ZnSn-0.5
CCE	2.8%	3.3%	3.4%	3.4%

According to reported work [10], carbon conversion efficiency (CCE) towards CO_2RR was calculated as a ratio of the molar amount of carbon following this equation:

$$CCE = \frac{n(CO) + n(HCOOH)}{n(CO_2) + n(TIC)} * 100\%$$

$n(CO)$: obtained from GC

$n(HCOOH)$: obtained from HPLC

$$n(CO_2) = \frac{pV}{RT}$$

p: 1 bar

R: 0.083144598 L bar mol^{-1} K^{-1}

V= v*t

v=20 mL/min

TIC: total inorganic carbon. In our work: TIC= 12 mmol and $n(CO_2)$= 7.5 mmol

Table S3. EE of the aqueous rechargeable Zn-CO_2 electrochemical cell

Current (mA)	Discharge voltage (V)	FE of CO_2 to HCOOH	FE of CO_2 to CO	Charge voltage (V)	FE of $H_2O \longrightarrow H_2+1/2O_2$	EE_1	EE_2
0.5	0.3316	58%	20%	2.44	10%	56.15%	61.5%
1	0.3196	60%	23%	2.5	8%	57.06%	61.19%
1.5	0.302	61%	23%	2.57	8%	55.19%	59.34%
2	0.2826	63%	26%	2.64	7%	55.65%	59.19%

Note: EE_1 is calculated based on CO_2 splitting in the cell, EE_2 is calculated when water splitting is also accounted for.

According to reported work [11], the energy efficiency (EE) of the cell calculated as follows:

$$EE_1 = \frac{\Delta G_{output}}{\Delta G_{input}} = \frac{nE_{discharge}F + FE_{CO\,+\,HCOOH} * \Delta G_{CO2\;splitting}}{nE_{charge}F}$$

$$EE_2 = \frac{\Delta G_{output}}{\Delta G_{input}} = \frac{nE_{discharge}F + FE_{CO\,+\,HCOOH} * \Delta G_{CO2\;splitting} + E_{H2} * \Delta G_{H2O\;splitting}}{nE_{charge}F}$$

$$\Delta G_{H2O\;splitting} = 257.38\ KJ\ mol^{-1}$$

$$\Delta G_{CO2\;splitting} = 257.38\ KJ\ mol^{-1}$$

Table S4. The atomic model of SnZn and Zn. Blue: Zn atoms; Yellow: Sn atoms; Red: H atoms; write: O atoms; grey: C atoms.

	SnZn	Zn
	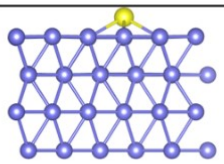	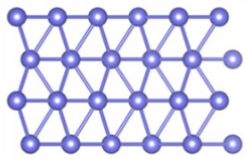
H^*	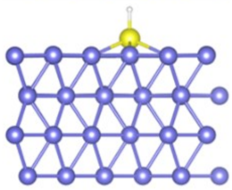	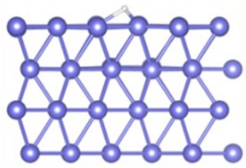
$^*COOH$	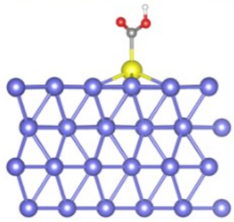	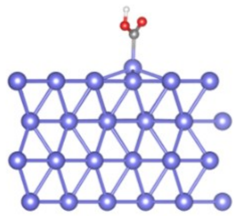
$^*OCOH$	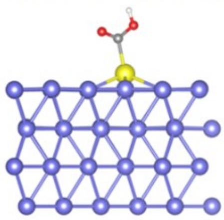	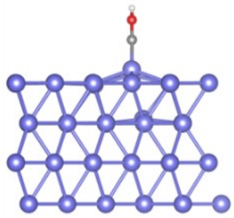
$^*OOCH$	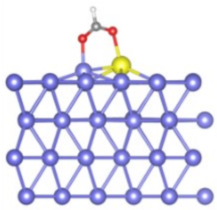	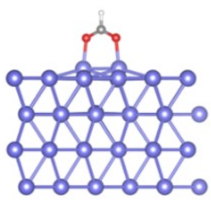

References

1. Mosali VSS, Zhang X, Zhang Y, et al. Electrocatalytic CO_2 Reduction to Formate on Cu Based Surface Alloys with Enhanced Selectivity. *ACS Sustainable Chemistry & Engineering.* 2019, 7, 19453-19462.
2. Liu W, Zhang Z, Huo S, et al. Bimetallic Zn_3Sn_2 electrocatalyst derived from mixed oxides enhances formate production towards CO_2 electroreduction reaction. *Appl Surf Sci.* 2023, 608, 155110.
3. Mohamed AGA, Zhou E, Zeng Z, et al. Asymmetric Oxo-Bridged ZnPb Bimetallic Electrocatalysis Boosting CO_2 - to - HCOOH Reduction. *Adv Sci (Weinh).* 2021, e2104138.
4. Zhang T, Qiu Y, Yao P, et al. Bi-Modified Zn Catalyst for Efficient CO_2 Electrochemical Reduction to Formate. *ACS Sustainable Chemistry & Engineering.* 2019, 7, 15190-15196.
5. Choi SY, Jeong SK, Kim HJ, et al. Electrochemical Reduction of Carbon Dioxide to Formate on Tin–Lead Alloys. *ACS Sustainable Chemistry & Engineering.* 2016, 4, 1311-1318.
6. Wang ZT, Qi RJ, Liu DY, et al. Exfoliated Ultrathin $ZnIn_2S_4$ Nanosheets with Abundant Zinc Vacancies for Enhanced CO_2 Electroreduction to Formate. *Chemsuschem.* 2021, 14, 852-859.
7. Kwon IS, Debela TT, Kwak IH, et al. Selective electrochemical reduction of carbon dioxide to formic acid using indium–zinc bimetallic nanocrystals. *J Mater Chem A.* 2019, 7, 22879-22883.
8. Rasul S, Pugnant A, Xiang H, et al. Low cost and efficient alloy electrocatalysts for CO_2 reduction to formate. *Journal of CO_2 Utilization.* 2019, 32, 1-10.
9. Zhang, Y.; Jang, H.; Ge, X.; Zhang, W.; Li, Z.; Hou, L.; Zhai, L.; Wei, X.; Wang, Z.; Kim, M. G.; Liu, S.; Qin, Q.; Liu, X.; Cho, J., Single-Atom Sn on Tensile-Strained ZnO Nanosheets for Highly Efficient Conversion of CO_2 into Formate. *Adv. Energy Mater.* 2022. 12, 2202695.
10. Izadi, P.; Song, J.; Singh, C.; Pant, D.; Harnisch, F., Assessing the Electrochemical CO_2 Reduction Reaction Performance Requires More Than Reporting Coulombic Efficiency. *Advanced Energy and Sustainability Research* 2024, *5*, 2400031
11. Wang, X.; Xie, J.; Ghausi, M. A.; Lv, J.; Huang, Y.; Wu, M.; Wang, Y.; Yao, J., Rechargeable Zn-CO_2 Electrochemical Cells Mimicking Two-Step Photosynthesis. Adv. Mater. 2019, e1807807.